Plant Cell Rep
DOI 10.1007/s00299-014-1574-y

ORIGINAL PAPER

Cell wall polysaccharide distribution in *Miscanthus lutarioriparius* stem using immuno-detection

Yingping Cao · Junling Li · Li Yu · Guohua Chai · Guo He · Ruibo Hu · Guang Qi · Yingzhen Kong · Chunxiang Fu · Gongke Zhou

Received: 8 January 2014 / Revised: 18 January 2014 / Accepted: 20 January 2014

Abstract

Key message **Cell wall polysaccharides' occurrences in two internodes of different development stages in *M. lutarioriparius* stem were analyzed and three major differences between them were identified by cell wall polysaccharide probes.**

Abstract Deposition and modification of cell wall polysaccharides during stem development affect biomass yield of the *Miscanthus* energy crop. The distribution patterns of cell wall polysaccharides in the 2nd and the 11th internodes of *M. lutarioriparius* stem were studied using in situ immunofluorescence assay. Crystalline cellulose and xylan were present in most of the stem tissues except phloem, where xyloglucan was the major composition of hemicellulose. The distribution of pectin polysaccharides varied in stem tissues, particularly in vascular bundle elements. Xylogalacturonan, feruloylated-1,4-β-D-galactan and (1,3)(1,4)-β-glucans, however, were insufficient for antibodies binding in both internodes. Furthermore, the distribution of cell wall polysaccharides was differentiated in the two internodes of *M. lutarioriparius*. The significant differences in the pattern of occurrence of long 1,5-α-L-arabinan chain, homogalacturonan and fucosylated xyloglucans epitope were detected between the two internodes. In addition, the relationships between probable functions of polysaccharides and their distribution patterns in *M. lutarioriparius* stem cell wall were discussed, which would be helpful to understand the growth characteristics of *Miscanthus* and identify potential targets for either modification or degradation.

Keywords Biofuel · Cell wall · Glycan-directed probes · In situ immunofluorescence assay · *M. lutarioriparius*

Communicated by Q. Zhao.

Y. Cao and J. Li contributed equally to the article.

Y. Cao · J. Li · L. Yu · G. Chai · G. He · R. Hu · G. Qi · C. Fu (✉) · G. Zhou (✉)
Key Laboratory of Biofuels, Chinese Academy of Sciences, Shandong Provincial Key Laboratory of Energy Genetics, Qingdao Institute of BioEnergy and Bioprocess Technology, Chinese Academy of Sciences (QIBEBT-CAS), Qingdao 266101, Shandong, People's Republic of China
e-mail: fucx@qibebt.ac.cn

G. Zhou
e-mail: zhougk@qibebt.ac.cn

Y. Kong
Key Laboratory of Tobacco Genetic Improvement and Biotechnology, Tobacco Research Institute of Chinese Academy of Agricultural Sciences, Qingdao 266101, People's Republic of China

Introduction

Plant cells synthesize their cell walls to build the shape of different cell types, fulfill important functions in intercellular communication, provide protection against mechanical stress and prevent attack from pathogen and disease (Keegstra 2010). Plant cell walls are principal features of plant cells distinct from animal cells and represent the major component of terrestrial biomass. Two types of cell walls, primary and secondary, are present in flowering plants. Primary cell wall is thin and flexible and predominantly composed of cellulose, hemicellulose and pectin. Secondary cell wall is thick and rigid and consists largely of cellulose, hemicellulose and lignin (Keegstra 2010). The bulk of lignocellulose stored in plant cell walls has been considered as an important renewable source for biofuel production (Doblin et al. 2010; Sticklen 2008). Therefore, the highly complex composites of structurally diverse

Published online: 13 February 2014

polysaccharides in cell walls have attracted considerable interest due to their important biological functions and agricultural value as biofuel and forage feedstock (Pauly and Keegstra 2010).

Cell wall polysaccharides mainly consist of cellulose, hemicellulose and pectin. Each polysaccharide class contains diverse domains or structures. Cellulose, as the major component of plant cell wall, is a linear polymer of β-1,4-linked glucose residues. Cellulose chains are cross-linked via intermolecular hydrogen bonds to form insoluble microfibril which is a mixture of crystalline and amorphous cellulose (Burton et al. 2010; Somerville 2006). Hemicellulose is the second most abundant polysaccharide in cell walls and can be divided into four general classes, i.e., xyloglucans, which contain a heavily substituted β-1,4-glucan backbone; xylans, comprising a substituted β-1,4-linked xylan backbone; (gluco)mannans, consisting of a variably substituted backbone that includes β-1,4-linked mannose (glucose and mannose) residues, and mixed-linkage glucans (MLG), containing both β-1,3- and β-1,4-linkages (Scheller and Ulvskov 2010). The third major class of cell wall polysaccharides is pectin. This class is a complex group of polymers, including homogalacturonan (HG) (with partially methyl-esterified and acetylated at the backbone), rhamnogalacturonan I (RGI) (comprising 1,4-β-D-galactan and 1,5-α-L-arabinan as side branches), the substituted galacturanans rhamnogalacturonan II (RGII), and xylogalacturonan (XGA) (Mohnen 2008).

The relationship between local cell wall components and the responses of tissues and organs to developmental signals for internal and external stimuli have been widely studied by immunochemical analysis with glycan-directed probes (Blake et al. 2008; Donaldson and Knox 2012; Sun et al. 2011). For example, the signal of less methyl-esterified HG recognized by JIM5 monoclonal antibody shows stronger intensity in the basal cortical than upper cortical of *Arabidopsis* stem, and the *pme35-1* mutant involved in demethylesterification of HG in the basal cortical exhibits a pendant stem phenotype, suggesting that ME (methyl esterification) degree of HG could regulate the mechanical strength of *Arabidopsis* stem (Hongo et al. 2012). The presence or absence of weakly ME-HGs and fucosylated xyloglucans in intervessel pit membranes might contribute to Pierce's disease susceptibility in grapevine (Sun et al. 2011). Changes in the amount and distribution of noncellulosic polysaccharides could mediate lignification and microfibril orientation of Radiata Pine wood (Donaldson and Knox 2012).

Miscanthus, a C4 perennial rhizomatous grass, has recently emerged as one of the leading dedicated bioenergy crops because of its high biomass yield, relatively low input requirement (Hodgson et al. 2010) and remarkable adaptability to different environments (Qin et al. 2012). Previous research indicated that *Miscanthus* possessed typical type II cell walls and had a high proportion of cellulose and xylan, 30–55 % and 13–30 % of total mass, respectively, depending on different species and harvest date and a correspondingly low content of pectin and xyloglucan (Allison et al. 2011; Heaton et al. 2010; Le Ngoc Huyen et al. 2010; Qin et al. 2012; Lygin et al. 2011). Among the *Miscanthus* species, *M. lutarioriparius* has been identified as an excellent candidate because of its high cellulose content and low total ash in cell walls (Qin et al. 2012) as well as its great productive potential even in unfavorable soil and climatic conditions (Sang and Zhu 2011). The temporal and spatial picture of cell walls polysaccharides organization during *Miscanthus* stem development, however, has yet to be elucidated.

In this paper, we used in situ immunofluorescence assay to analyze cell wall polysaccharides' occurrences in *M. lutarioriparius* stem where the major lignocellulosic biomass accumulated. The comprehensive distribution patterns of cell wall polysaccharides were drawn using 20 glycan-directed probes which recognized the epitopes of cellulose, hemicellulose and pectin in *M. lutarioriparius* stem. Given the fact that chemical properties of cell walls are varied at developmental stages, the 2nd internode and 11th internode numbered from the bottom of *M. lutarioriparius* stem were selected to detect the differences between them. The distinction of cell wall polysaccharides occurrence between internodes of *M. lutarioriparius* has here been documented for the first time, suggesting the diverse functions of the polysaccharide polymers during the process of internode development.

Materials and methods

Plant materials

M. lutarioriparius was grown by planting rhizome in the growth chamber for 2 months at 20–24 °C with a 16 h light per day and relative humidity 55 %. The development stages of *M. lutarioriparius* are defined as described by Moore et al. (1991). The 11th (top) and 2nd (bottom) internodes were harvested from the plants at E11 stage (Elongation-stem comprising 11 internodes) and employed for in situ immunofluorescence assay.

Monoclonal antibodies

The monoclonal antibodies used in this study and their corresponding antigen/epitopes are described in Table 1. Briefly, CBM3a (CBM, carbohydrate-binding module) and CBM17 bind to epitopes of cellulose. LM10, LM11, LM15, LM21 and CCRC-M1, CCRC-M54, CCRC-M99 together with anti-MLG monoclonal antibody bind to

Table 1 Cell wall glycan-directed probes used in the study of in situ analysis of *M. lutarioriparius* stem

Probes	Monoclonal antibodies	Antigen/epitopes	References
Cellulose	CBM3a	Crystalline cellulose	Altaner et al. (2007)
	CBM17	Amorphous cellulose	Altaner et al. (2007)
Hemicellulose	(Glucuronoarabino)xylans		
	LM10	Unsubstituted xylan/low-substituted xylans	McCartney et al. (2005)
	LM11	Arabinoxylan/unsubstituted xylan	McCartney et al. (2005)
	Xyloglucans		
	LM15	Non-fucosylated xyloglucan (XXXG)	Marcus et al. (2008)
	CCRC-M54	Non-fucosylated xyloglucan (XLLG)	Young et al. (2008) and Pattathil et al. (2010)
	CCRC-M99	Non-fucosylated xyloglucan (XLLG)	http://glycomics.ccrc.uga.edu/wall2/jsp/abdetails.jsp?abnumber=152&abname=CCRC-M99
	CCRC-M1	Fucosylated xyloglucans	Pattathil et al. (2010)
	(Gluco)mannans		
	LM21	Mannans	Marcus et al. (2010)
	Mixed-linkage glucans		
	Anti-MLG monoclonal antibody	(1,3)(1,4)-β-Glucans	Meikle et al. (1994)
Pectin	Homogalacturonan (HG)		
	LM19	Partially ME-HG/de-esterified HG	Verhertbruggen et al. (2009)
	JIM5	Partially ME-HG	Willats et al. (2001)
	JIM7	Partially ME-HG	Willats et al. (2001)
	LM20	Partially ME-HG	Verhertbruggen et al. (2009)
	Rhamnogalacturonan I (RGI) related		
	LM5	(1-4)-β-D-Galactan	Jones et al. (1997)
	LM9	Feruloylated-(1,4)-β-D-galactan	Clausen et al. (2004)
	LM6	(1-5)-α-L-arabinan	Verhertbruggen et al. (2009)
	LM13	Linearized-(1,5)-α-L-arabinan	
	LM16	Processed arabinan	
	Xylogalacturonan (XGA)		
	LM8	Xylogalacturonan	Willats et al. (2004)

epitopes of hemicellulose. LM5, LM6, LM8, LM9, LM13, LM16, LM19 and LM20 together with JIM5 and JIM7 bind to epitopes of pectin.

Sample fixation

Internode samples were cut into 0.5–1.0 cm pieces and subsequently fixed in 70 % (v/v) ethanol, 5 % (v/v) formaldehyde, 5 % (v/v) glacial acetic acid, and dehydrated by passing through an ethanol and a xylene series. The xylene was gradually replaced by Paraplast plus chips (Sigma, MO, USA) at 60 °C, and finally the internode sections were embedded in paraplast plus boxes and stored at 4 °C. The above pieces were cut to 8 μm thickness sections and placed on lysine-treated slides which were dried for two days at 42 °C, and de-waxed with xylene and hydrated through an ethanol series (100 to 0 %).

Immunolabelling procedures

CCRC antibodies were prepared from a threefold dilution of monoclonal antibody hybridoma cell culture supernatant, LM and JIM antibodies were subjected to a tenfold dilution, and the anti-MLG monoclonal antibody (Biosupplies, VIC, Australia) was diluted to 20 μg/ml, respectively, using 3 % MP/PBS. Sections of *M. lutarioriparius* internode were incubated in 3 % MP/PBS for 1 h followed by the above monoclonal antibody hybridoma cell culture supernatant for 2 h. Samples were washed three times (5 min each time) in 3 % PBS and incubated with a 100-fold dilution of anti-mouse-IgG for the CCRC and anti-MLG monoclonal antibody or anti-rat-IgG for LM and JIM antibodies in the dark for 1 h.

To detect CBM3a binding, internode sections were incubated in 3 % MP/PBS containing 10 μg/ml CBM3a for 2 h. After washing with PBS, the sections were incubated with a

100-fold dilution of mouse anti-his monoclonal antibody for 1.5 h. Then, the sections were washed three times in PBS (5 min each time) and incubated with anti-mouse-IgG in the dark for 1 h. All the above anti-mouse/rat-IgG antibodies were linked to FITC (Fluorescein-isothiocyanate), and the entire process was performed at 28 °C (Yu et al. 2011).

Immunofluorescence detection

The immunolabeled samples were washed three times (5 min each) with PBS after immunolabelling procedures and were stained with 0.25 μg/ml Calcofluor White M2R (Fluorescent Brightener 28, Sigma, MO, USA) for 5 min and then washed three times (5 min each time) with PBS. Immunofluorescence and staining sections were observed with an Olympus BX-51 microscope with U-MWV2 filter cube (excitation: 330–385 nm, emission: 420 nm, Dichromatic: 400 nm, applicable fluorochrome: calcofluor white) and U-MWIBA2 filter cube (excitation: 460–490 nm, emission: 510–550 nm, Dichromatic: 505 nm, applicable fluorochrome: FLTC). Fluorescence images generated with Calcofluor White staining (blue) and monoclonal antibodies to their corresponding epitopes (green) were documented and overlapped with Volocity software (PerkinElmer, CA, USA).

Histochemical staining of lignin

The 11th and 2nd internode samples of *M. lutarioriparius* were collected and prepared for microscopy as described above. Lignin was detected by phloroglucinol-HCl method as described by Melton and Smith (2001).

Results

Anatomy of the *M. lutarioriparius* stem

Histochemical staining of lignin showed that *M. lutarioriparius* stem consisted of various tissues, such as parenchyma, vascular bundles and sclerenchyma fibers (Fig. 1). The 2nd internode was hollow because its center parenchyma had dried out and disintegrated (Fig. 1a). The sieve tubes and companion cells formed a regular pattern in phloem. The pitted vessels and protoxylem vessels arranged in the shape of "Y" in xylem (Fig. 1b, d). Lacunae were formed because cell walls of some annular vessels were ripped apart by the internode's continuative elongation (Fig. 1a, b) (Dong et al. 1997). The vascular bundles were well lignified in the 2nd internode (Fig. 1a, b). Significant cell wall lignification, however, was only observed in protoxylem vessels of the 11th internode (Fig. 1c, d).

Cellulose distribution in *M. lutarioriparius* stem

CBM3a and CBM17 were two antibodies directed to crystalline cellulose and amorphous cellulose, respectively (Table 1). In situ immunofluorescence assay revealed that CBM3a epitope was abundant in the cell walls of most tissues in the 11th and 2nd internodes except phloem tissue (Fig. 2). The discontinuous gap of its labeling signals in pitted vessels reflected the pit membrane locations (white arrow in Fig. 2). In contrast, CBM17 did not bind to the cell walls of either internode.

Hemicellulose distribution in *M. lutarioriparius* stem

Eight monoclonal antibodies were employed to study the distribution of hemicellulose polysaccharides in *M. lutarioriparius* stem. Xylans were detected by LM10 and LM11 antibodies in *M. lutarioriparius* stem. LM10 is specific to unsubstituted or low-substituted xylans, whereas LM11 binds to both arabinoxylan and unsubstituted xylans (Table 1). LM10 epitope was observed in sclerenchyma fibers, vascular bundles and epidermis in transverse sections of both internodes (Fig. 3a, b). It was detected in the center sclerified parenchyma cell walls of the 11th internode as well (Fig. 3b). LM11 bound to the most cell walls of parenchyma and vascular bundle

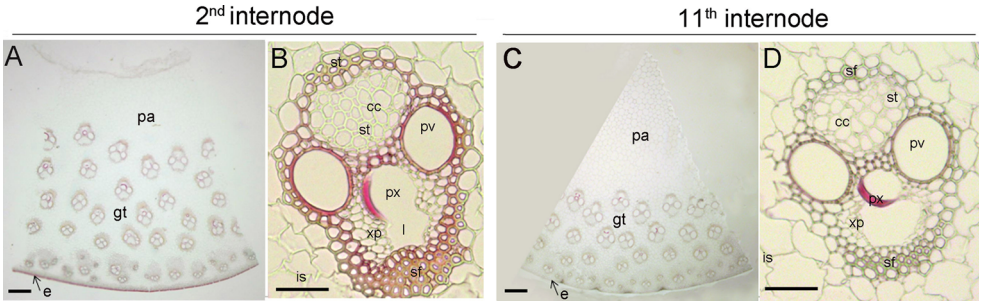

Fig. 1 Transverse section of *M. lutarioriparius* stem stained with phloroglucinol-HCl solution. **a**, **c** The transverse sections of the 2nd internode and the 11th internode, respectively. **b**, **d** The vascular bundle in a and c, respectively. *pa* parenchyma cells, *cc* companion cells, *st* sieve tube, *pv* pitted vessel, *px* protoxylem, *is* intercellular space, *xp* xylem parenchyma, *sf* sclerenchyma fibers, *gt* ground tissue, *e* epidermis. *Scale bar* 200 μm in **a** and **c**, *scale bar* 50 μm in **b** and **d**

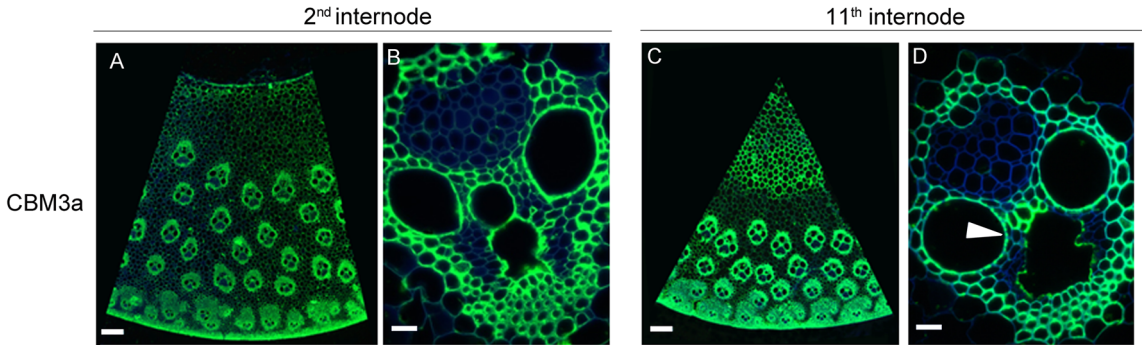

Fig. 2 Immunofluorescence analysis of crystalline cellulose epitope in transverse sections of *M. lutarioriparius* stem by CBM3a. **a**, **c** The transverse sections of the 2nd internode and the 11th internode, respectively. **b**, **d** The vascular bundle in the corresponding sections. The *white arrow* showed the pit membranes. *Scale bar* 200 μm in **a** and **c**, *scale bar* 20 μm in **b** and **d**

tissues of *M. lutarioriparius* internodes (Fig. 3c, d). In some cases, intercellular spaces of ground tissue cells were filled with LM11 epitope in the 2nd internode (yellow arrow and white box in Fig. 3c). It is likely that unsubstituted or low-substituted xylans tend to be deposited in sclerenchyma fibers and sclerified parenchyma cell walls.

The distribution patterns of mannans were revealed by the LM21 probe. LM21 assay showed a punctate manner throughout the whole section in *M. lutarioriparius* internodes (Fig. 3e, f). The anti-MLG monoclonal antibody directed to (1,3)(1,4)-β-glucans was used to determine the occurrence of mix-linked glucans in *M. lutarioriparius* stem. No cell walls were labeled by the antibody in *M. lutarioriparius* stem.

Xyloglucans were detected in *M. lutarioriparius* stem. Xyloglucan is composed of (1,4)-β-linked glucan backbone regularly substituted at C6 with xylose residues, longer side chains also occur and a single letter code is used to describe their compositions. LM15, CCRC-M54 and CCRC-M99 were employed to label non-fucosylated xyloglucan motifs. Among them, LM15 recognizes XXXG motif (Hsieh and Harris 2009; Marcus et al. 2008), and CCRC-M54 and CCRC-M99 recognize XLLG motif (Hsieh and Harris 2009; Pattathil et al. 2010; Young et al. 2008). LM15, CCRC-M54 and CCRC-M99 assay showed similar binding patterns, and their epitopes were all observed in phloem cell walls (Fig. 4a–f). In some cases, these antibodies bound to pit membranes and cell walls around the lacunae in xylem (yellow and purple arrows in Fig. 4e). CCRC-M1 was used to detect the fucosylated xyloglucans motif. CCRC-M1 revealed the difference in occurrence between the 11th internode and 2nd internode. CCRC-M1 epitope was clearly detected in all phloem cells in the 11th internode. However, the strong signals were only observed in some sieve tubes, but not all phloem cells in the 2nd internode (Fig. 4g, h).

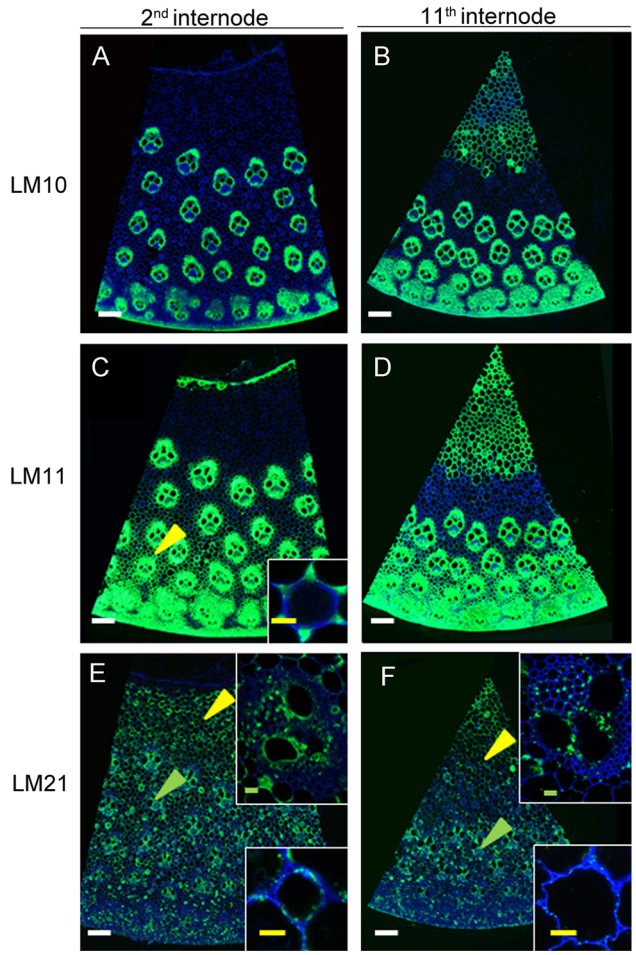

Fig. 3 Immunofluorescence analysis of (arabino)xylan and mannans in transverse sections of *M. lutarioriparius* stem by LM10 (unsubstituted or low-substituted xylans), LM11 ((arabino)xylan and low-substituted xylans) and LM21 (mannans) antibodies. **a**, **c**, **e** The transverse sections of the 2nd internode, and **b**, **d**, **f** the transverse sections the 11th internode. **a**, **c** The equivalent section to **e**, while **b** and **d** were the equivalent section to **f**. The *colorized arrow* position was magnified in the *box* with the *same color scale bar*. *White scale bar* 200 μm in **a**–**f**; *colorized scale bar* 20 μm in *white box pictures* (color figure online)

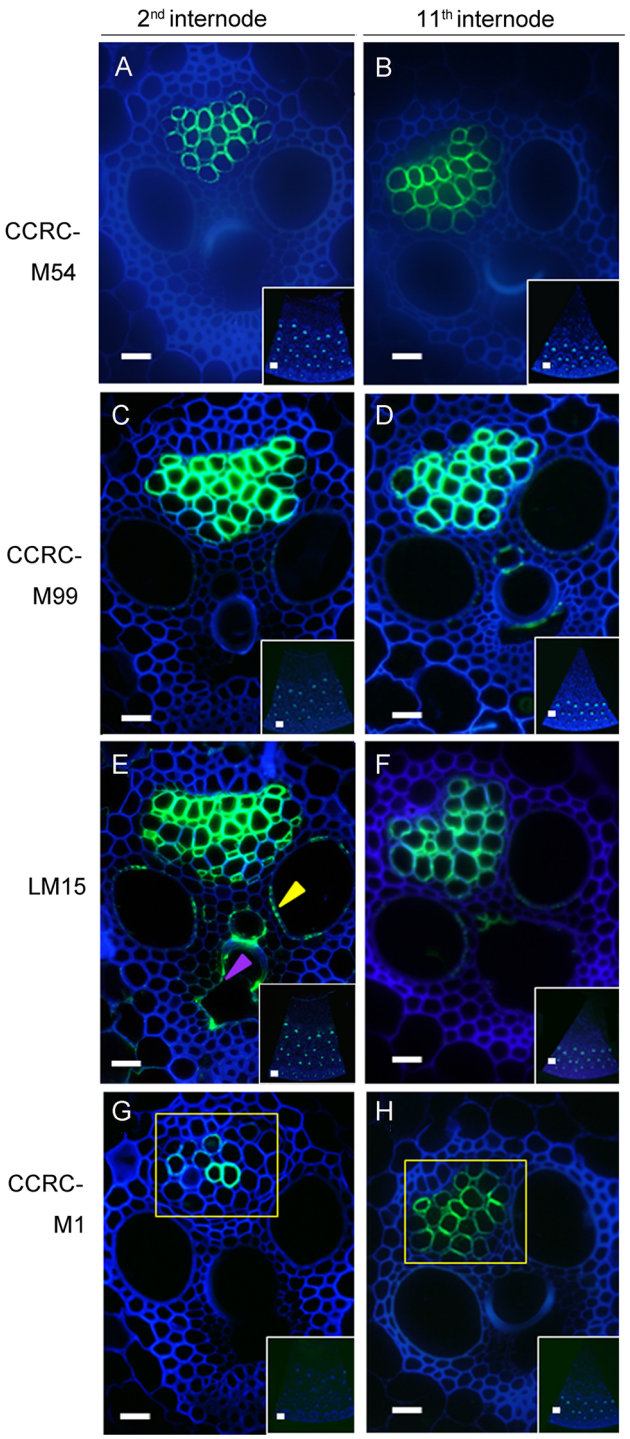

◀**Fig. 4** Immunofluorescence analysis of xyloglucan motifs in transverse sections of *M. lutarioriparius* stem by CCRC-M54 (XLLG), CCRC-M99 (XLLG), LM15 (XXXG), and CCRC-M1 (fucosylated xyloglucan) antibodies. **a**, **c**, **e**, **g** The transverse sections of the 2nd internode while **b**, **d**, **f**, **h** the transverse sections of the 11th internode. The *white box* in each photo showed the immunofluorescence analysis of whole transverse sections, vascular bundle in the transverse section was magnified in the same photo. *Yellow arrows* showed pit membranes and purple arrows showed lacuna. *Yellow boxes* in **g** and **h** showed the different occurrence pattern of CCRC-M1 epitope between the two internodes. **a**, **c**, **e** Were the equivalent section to **g**, while **b**, **d** and **f** were the equivalent section to **h**. *Scale bar* 20 μm in **a**–**h**; *scale bar* 200 μm in the picture of *white boxes* (color figure online)

Distribution of pectic polysaccharides in *M. lutarioriparius* stem

HG is a multifunctional pectic polysaccharide in the primary cell wall matrix of all land plants. JIM5, JIM7, LM19 and LM20 were used to exhibit HG distribution in *M. lutarioriparius* stem. The above antibodies can distinguish HG with different ME rates, among which LM19 was proved to be the only antibody that bound to no methyl-esterified HG as well as the partially methyl-esterified HG (Verhertbruggen et al. 2009). Their binding patterns, however, were similar in the ground tissues of *M. lutarioriparius* stem. The corresponding epitopes were observed in the most cell wall linings of intercellular spaces (Fig. 5a–d, i–l). In vascular region, the above antibodies bound to the cell walls around the lacunae (or protoxylem vessels) and phloem cells with varied degrees (Fig. 5e–h, m–p). Among them, JIM7 HG epitope had a broad distribution in sieve tube and companion cells of phloem tissue (Fig. 5f, n), the middle lamella of sclerenchyma fibers (purple arrows in Fig. 5b, j) and the lining of intercellular spaces in ground tissues (yellow arrows in Fig. 5b, j). Different binding patterns between the two internodes were found in the center parenchyma (light green arrows in Fig. 5), unlike occurrence in the lining of intercellular space in 11th internode (light green arrows in Fig. 5i–l); the distribution patterns of partially methyl-esterified HGs recognized by JIM5, JIM7 and LM20 were restricted to the corners (light green arrows Fig. 5a–c); in contrast, the distribution of partially Me-HG/HG recognized by LM19 extended to the whole cell wall of parenchyma cells in the 2nd internode (light green arrow Fig. 5d), which implied that there were more partially/de-esterified HG in the 2nd internode than in the 11th internode in center parenchyma.

In higher plants, 1,4-β-D-galactan, 1,5-α-L-arabinan and related pectic polysaccharides are usually thought to occur predominantly in the side chains of RG-I. LM5, LM6, LM13 and LM16 were employed to detect RG-I related domains in the cell walls of *M. lutarioriparius* stem. The epitopes of LM6 (short 1,5-α-L-arabinan chain), LM16 (processed arabinan) and LM5 (1,4-β-D-galactan) had similar distribution patterns in all regions except phloem in both internodes. They were detected in the most parenchyma cell walls and in the inner region of secondary cell walls (Fig. 6a–c, i–k; white arrows and white boxes in Fig. 6e–g, m–o). Their binding patterns, however, were distinct in the phloem. LM6 labeled

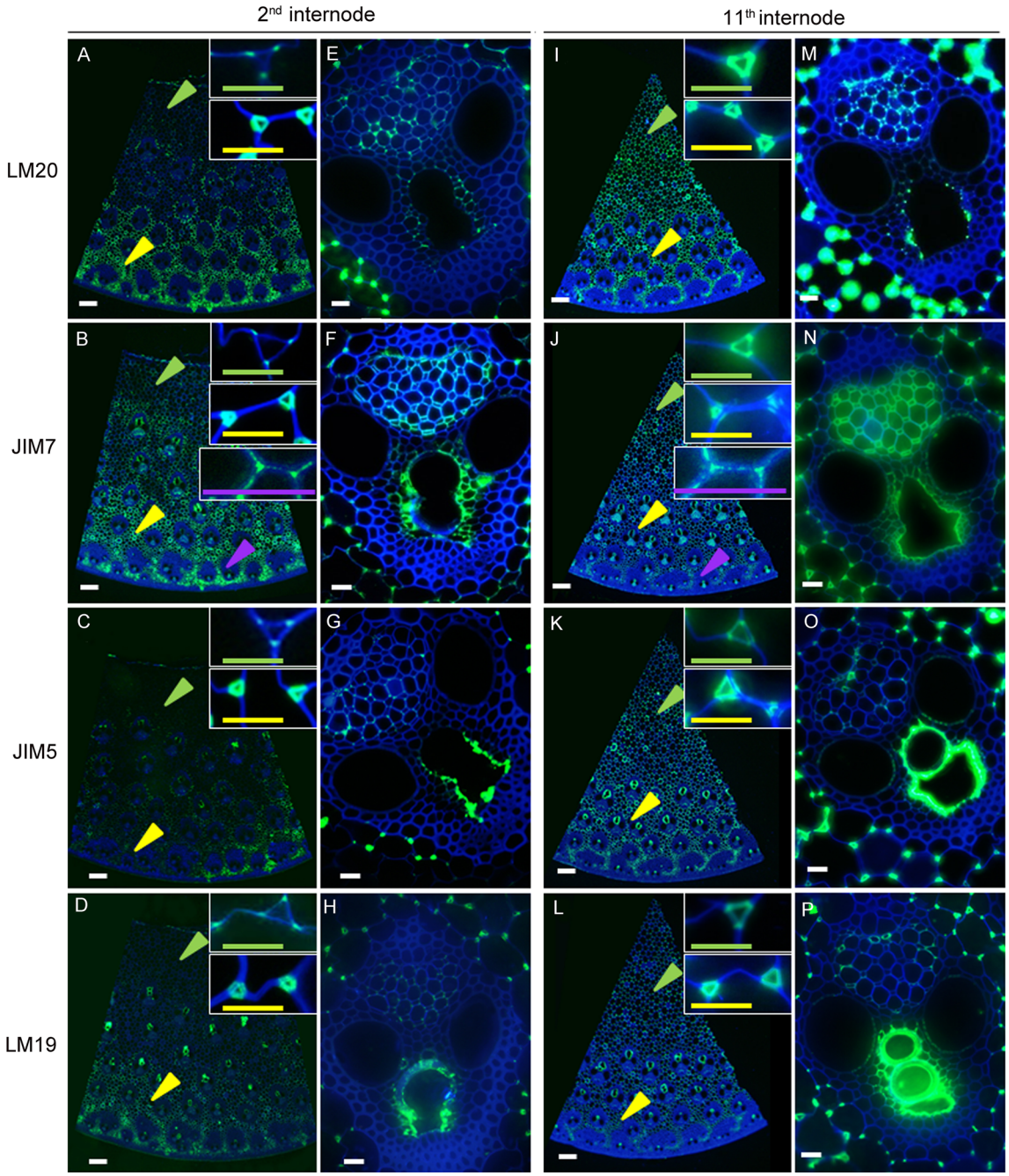

Fig. 5 Immunofluorescence analysis of HG in transverse sections of *M. lutarioriparius* stem by LM20 (Partially ME-HG), JIM7 (Partially ME-HG), JIM5 (Partially ME-HG) and LM19 (Partially ME-HG/de-esterified HG) antibodies. **a**–**h** The transverse sections of the 2nd internode while **i**–**p** showed the transverse sections of the 11th internode. The vascular bundles in the corresponding sections were shown in the *right row* (**e**–**h** and **m**–**p**). The *colorized arrow* positions were magnified in the *box* with the *same color scale bar*. **a**–**c** Were the equivalent section to **e**, while **i**–**k** were the equivalent section to **l**. *White scale bar* in **a**–**d** and **i**–**l** 200 μm; other *scale bars* (including colorized *scale bar* in **a**–**d** and **i**–**l**) 20 μm (color figure online)

weakly to phloem cell walls (Fig. 6e, m). LM5 galactan epitope was only detected in companion cell walls (Fig. 6f, n). LM16 epitope was abundant in both sieve tube and companion cells (Fig. 6g, o).

The long 1,5-α-L-arabinan chain recognized by LM13 was mainly observed in the xylem of vascular bundles. Particularly in the cell walls around the lacunae (protoxylem vessels) and pit membranes, it was detected in adherent region of center parenchyma cells in some cases (Fig. 6h, p; white arrows in Fig. 6d, l). Feruloylated galactan and XGA recognized by LM9 and LM8 antibodies, respectively, however, were not detected in either internode.

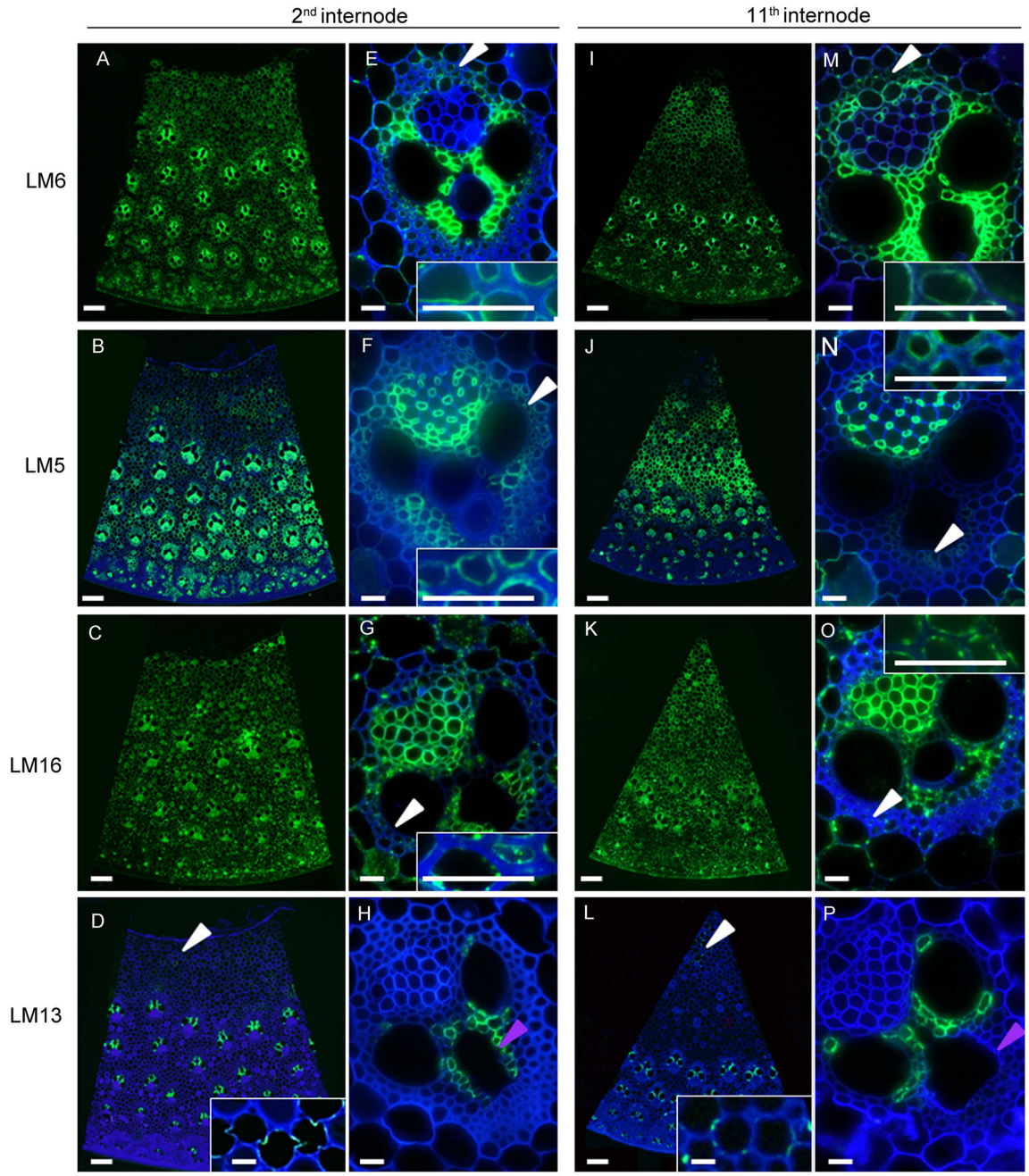

Fig. 6 Immunofluorescence detections of RGI related polymers in transverse sections of *M. lutarioriparius* stem by LM6 (short 1,5-α-L-arabinan chain), LM5 (1,4-β-D-galactan), LM16 (processed arabinan) and LM13 (long 5-α-L-arabinan chain) antibodies. **a**–**h** The transverse sections of the 2nd internode while **i**–**p** showed the transverse sections of the 11th internode. The vascular bundles in the corresponding sections were shown in the *right rows* (**e**–**h** and **m**–**p**). The *white arrow* positions were magnified in *white box* in the same photo. **a**–**c** Were the equivalent section to **e**, while **i**–**k** were the equivalent section to **l**. *Scale bar* 200 μm in **a**–**d**, **i**–**l**; *scale bar* 20 μm in other pictures (including the *white box*)

Moreover, the notably different distributions of the above four epitopes were observed between the two internodes. LM13 epitope, long 1,5-α-L-arabinan chain, was rarely detectable in cell walls around protoxylem vessels (the lacunae) in the 11th internode but was abundant in the same position of the 2nd internode (purple arrows in Fig. 6h, p).

Discussion

M. lutarioriparius, a new species resembling *M. sacchariflorus*, has the highest biomass yield among the major *Miscanthus* species widely grown in China (Sang and Zhu 2011). *M. lutarioriparius* possesses lignocellulosic biomass

which can be converted to fuels, such as ethanol, butanol, and methane. Cell wall structure and composition affect biofuel production of lignocellulosic materials (Lygin et al. 2011). Here, we investigated cell wall polysaccharides composition and distributions in *M. lutarioriparius* internodes and provided valuable information for basic understanding of stem development characteristics in *Miscanthus*.

The individual internodes along the stem of *M. lutarioriparius* roughly represent the gradual process of cell wall lignification (Sarath et al. 2007). Histochemical staining of lignin demonstrated that the 2nd internode was well developed and lignified compared with the 11th internode at E11 stage (Fig. 1). Arabinoxylans form cross-links between lignin and cellulose and contribute to cell mechanical properties in type II cell walls (Carpita and Gibeaut 1993). Our results indicated that cell walls of *M. lutarioriparius* stem had a high content of cellulose and xylan with a wide distribution throughout all of the tissues (Figs. 2, 3c, d). By contrast, the bulk of xyloglucans was restricted to phloem tissues (Fig. 4). Thus, *M. lutarioriparius* cell wall was classified as type II cell wall (Heaton et al. 2010). The occurrence of MLG in type II cell walls has been reported in the cell walls of the leaves of various *Poaceae* species, such as *Lolium multiflorum* (Trethewey et al. 2005), barley (Burton and Fincher 2009), rice (Vega-Sánchez et al. 2012), and three *Miscanthus* ecotype seedlings, where MLG content increased during cold acclimation (Domon et al. 2013). The trace of MLG, however, was undetectable in the stem of *M. lutarioriparius* in the present study. It is likely that MLG have varied distribution in different tissues, organs or development stage of *Miscanthus* species.

CCRC-M1 is a monoclonal antibody employed to recognize fucosylated xyloglucans. Our results clearly demonstrated that a low amount of fucosylated xyloglucans were accumulated in the phloem of the 2nd internode compared with the 11th internode (Fig. 4h, g). The fucosylated xyloglucans motif occurrence in cell walls of monocot species has been systematically studied using CCRC-M1 antibody, revealing that the fucosylated xyloglucans motif occurs in both sieve tube and companion cell walls of the phloem in *Poaceae* species (Brennan and Harris 2011), which was similar to that observed in the 11th internode of *M. lutarioriparius*. However, the fact that CCRC-M1 labeling region was largely reduced in phloem of the 2nd internode and restricted, in most cases, to the sieve tube elements was intriguing. Fucosylated xyloglucans can inhibit auxin-stimulated growth in the plant stem only in an appropriate concentration range, higher than that in the observed range; fucosylated xyloglucans failed to antagonize auxin-induced growth (Augur et al. 1992; York et al. 1984). The fact that more CCRC-M1 epitopes were detected in the 11th internode implied an appropriate requirement for fucosylated xyloglucans during the process of internode elongation.

Pectins, including HG, RGI, RGII, and XGA, are structurally and functionally complex polysaccharides in plant cell walls that impact plant growth, morphology, development and defense (Mohnen 2008). Pectin level, however, is low in type II cell walls compared with type I cell walls (Burton et al. 2010). The clear functions of pectin in type II cell walls are underlying. The pectin distribution patterns in *M. lutarioriparius* stem were various (Figs. 5, 6) and implied their diverse roles in cell walls, particularly in vascular bundles. Vascular bundles play an important role to transport water, nutrients, hormones and wounding signals from one part to another in plant (Suzuki et al. 2002). Some pectic components were specifically distributed in vascular elements. For example, 1,4-β-D-galactan was present in companion cells of phloem (Fig. 6f, n), and long 1,5-α-L-arabinan chains were detected in xylems (Fig. 6h, p), suggesting their unique roles in these vascular elements.

LM13 epitope, long 1,5-α-L-arabinan chains, showed different occurrence patterns between the two internodes, which was rarely detectable in cells around the lacunae (protoxylem vessels) in the 11th internode of *M. lutarioriparius* but was abundant in these types of cells in the 2nd internode (purple arrows in Fig. 6h, p). Previous studies demonstrated that arabinans had coordinate functions with HG during stomata opening and closing processes. Degradation of cell wall arabinans prevented either stomata opening or closing. The locking of guard cell wall movements could be reversed if HG was subsequently removed from the walls. It implied that HG domains tended to form a tight gel and arabinans might play a role in maintaining flexibility of cell walls (Jones et al. 2003). In the present study, long arabinan chain and HG were co-localized in parenchyma cell walls around the lacunae or protoxylem vessels (Figs. 5, 6h, p). The cell walls of the protoxylem vessels were ripped apart after the differentiation of protoxylem vessels ceased and then the lacunae formed during the process of sugarcane internode elongation (Dong et al. 1997). The 11th internode was an immature internode differentiating from the shoot apical meristem (SAM). Most protoxylem vessel cell walls were intact and few lacunae were formed in this internode. The surrounding tissues of protoxylem vessels were required to maintain the protoxylem vessel shapes and, therefore, HG rather than arabinan was the major composition (Figs. 5, 6h, p). In contrast, the 2nd internode was a mature internode where the most protoxylem vessels were destroyed and more lacunae were formed during the process of internode elongation. Long 1,5-α-L-arabinan chain might play a role in protoxylem vessel's tearing process, and also might regulate the opening condition of lacunae to a shape of lowest energy by means of maintaining flexibility of cell walls as its function in stomata cells. Taken together, our results suggested that the substantially increased long arabinan chain in cell walls of the

2nd internode was involved in the process of protoxylem lacunae establishment.

The partially ME-HGs in cell walls of *M. lutarioriparius* were detected using LM20, JIM7 and JIM5. The occurrence of partial ME-HGs in the 11th internode was restricted to the lining of intercellular spaces in some center parenchyma cells (light green arrows in Fig. 5i–k). In contrast, the distribution region of partially ME-HGs in the cell walls of the 2nd internode was reduced to the corner of intercellular spaces (light green arrows in Fig. 5a–c). The binding region of LM19 that recognized partially Me-HG or de-esterified HG was expanded to the middle lamella of parenchyma cell walls in the 2nd internode (light green arrow in Fig. 5d) rather than restricted to the lining of intercellular spaces in the 11th internode (light green arrow in Fig. 5l). The demethylesterification of HG in the base stem of *Arabidopsis* can strengthen the support structure (Hongo et al. 2012). Thus, we suspected a similar function of partially Me/de-esterified HG in the strength of *M. lutarioriparius* stem.

In conclusion, 20 antibodies were employed to comprehensively investigate the distribution patterns of cellulose, hemicellulose and pectin in cell walls of *M. lutarioriparius* stem. The variations in cell wall polysaccharides are firstly documented here in *M. lutarioriparius* internodes with different lignification rates and can roughly represent the process of stem development. This elucidation of polysaccharide polymers occurrences in *M. lutarioriparius* stem provides a polysaccharide distribution model for herbaceous monocotyledons with type II cell walls, and understanding the growth characteristics of *Miscanthus* can ultimately lead to the identification of potential targets for improving yield and quality as a renewable material.

Acknowledgments LM and CBM series monoclonal antibodies were general gifts from Prof. J. Paul Knox (Centre for Plant Sciences, Faculty of Biological Sciences, University of Leeds, United Kingdom), and JIM and CCRC series monoclonal antibodies were gifts from Prof. Michael G. Hahn (Complex Carbohydrate Research Center, University of Georgia, USA). We would like to thank them for kindly providing monoclonal antibodies. The authors like to thank Amy Mason (Forage Improvement Division, the Samuel Roberts Noble Foundation, USA) for her critical review on the manuscript. Financial support for this work was obtained from the National Science and Technology Support Program (2013BAD22B01), the National Basic Research Program of China (2012CB114501), the National High-Tech Research and Development Program of China (2011AA100209) and the Program of 100 Distinguished Young Scientists of the Chinese Academy of Sciences (to Chunxiang Fu).

References

Allison GG, Morris C, Clifton-Brown J, Lister SJ, Donnison IS (2011) Genotypic variation in cell wall composition in a diverse set of 244 accessions of *Miscanthus*. Biomass Bioenergy 35:4740–4747

Altaner C, Knox JP, Jarvis MC (2007) In situ detection of cell wall polysaccharides in Sitka spruce (*Picea sitchensis* (Bong.) Carriere) wood tissue. Bioresources 2:284–295

Augur C, Yu L, Sakai K, Ogawa T, Sinaÿ P, Darvill AG, Albersheim P (1992) Further-studies of the ability of xyloglucan oligosaccharides to inhibit auxin-stimulated growth. Plant Physiol 99:180–185

Blake AW, Marcus SE, Copeland JE, Blackburn RS, Knox JP (2008) In situ analysis of cell wall polymers associated with phloem fibre cells in stems of hemp, *Cannabis sativa* L. Planta 228:1–13

Brennan M, Harris PJ (2011) Distribution of fucosylated xyloglucans among the walls of different cell types in monocotyledons determined by immunofluorescence microscopy. Mol Plant 4:144–156

Burton RA, Fincher GB (2009) (1,3;1,4)-β-D-glucans in cell walls of the Poaceae, lower plants, and fungi: a tale of two linkages. Mol Plant 2:873–882

Burton RA, Gidley MJ, Fincher GB (2010) Heterogeneity in the chemistry, structure and function of plant cell walls. Nat Chem Biol 6:724–732

Carpita NC, Gibeaut DM (1993) Structural models of primary cell walls in flowering plants: consistency of molecular structure with the physical properties of the walls during growth. Plant J 3:1–30

Clausen MH, Ralet MC, Willats WGT, McCartney L, Marcus SE, Thibault JF, Knox JP (2004) A monoclonal antibody to feruloylated-(1–4)-β-D-galactan. Planta 219:1036–1041

Doblin MS, Pettolino F, Bacic A (2010) Plant cell walls: the skeleton of the plant world. Funct Plant Biol 37:357–381

Domon JM, Baldwin L, Acket S, Caudeville E, Arnoult S, Zub H, Gillet F, Lejeune-Hénaut I, Brancourt-Hulmel M, Pelloux J, Rayon C (2013) Cell wall compositional modifications of *Miscanthus* ecotypes in response to cold acclimation. Phytochemistry 85:51–61

Donaldson LA, Knox JP (2012) Localization of cell wall polysaccharides in normal and compression wood of radiata pine: relationships with lignification and microfibril orientation. Plant Physiol 158:642–653

Dong Z, McCully ME, Canny MJ (1997) Does *Acetobacter diazotrophicus* live and move in the xylem of sugarcane stems? Anatomical and physiological data. Ann Bot 80:147–158

Heaton EA, Dohleman FG, Miguez AF, Juvik JA, Lozovaya V, Kader J-C, Delseny M (2010) *Miscanthus*: a promising biomass crop. Adv Bot Res 56:75–137

Hodgson EM, Lister SJ, Bridgwater AV, Clifton-Brown J, Donnison IS (2010) Genotypic and environmentally derived variation in the cell wall composition of *Miscanthus* in relation to its use as a biomass feedstock. Biomass Bioenergy 34:652–660

Hongo S, Sato K, Yokoyama R, Nishitani K (2012) Demethylesterification of the primary wall by PECTIN METHYLESTERASE35 provides mechanical support to the *Arabidopsis* stem. Plant Cell 24:2624–2634

Hsieh YS, Harris PJ (2009) Xyloglucans of monocotyledons have diverse structures. Mol Plant 2:943–965

Jones L, Seymour GB, Knox JP (1997) Localization of pectic galactan in tomato cell walls using a monoclonal antibody specific to (1-4)-β-D-galactan. Plant Physiol 113:1405–1412

Jones L, Milne JL, Ashford D, McQueen-Mason SJ (2003) Cell wall arabinan is essential for guard cell function. Proc Natl Acad Sci USA 100:11783–11788

Keegstra K (2010) Plant cell walls. Plant Physiol 154:483–486

Le Ngoc Huyen T, Rémond C, Dheilly RM, Chabbert B (2010) Effect of harvesting date on the composition and saccharification of *Miscanthus* × *giganteus*. Bioresour Technol 101:8224–8231

Lygin AV, Upton J, Dohleman FG, Juvik J, Zabotina OA, Widholm JM, Lozovaya VV (2011) Composition of cell wall phenolics and polysaccharides of the potential bioenergy crop—*Miscanthus*. GCB Bioenergy 3:333–345

Marcus SE, Verhertbruggen Y, Hervé C, Ordaz-Ortiz JJ, Farkas V, Pedersen HL, Willats WG, Knox JP (2008) Pectic homogalacturonan masks abundant sets of xyloglucan epitopes in plant cell walls. BMC Plant Biol 8:60

Marcus SE, Blake AW, Benians TAS, Lee KJD, Poyser C, Donaldson L, Leroux O, Rogowski A, Petersen HL, Boraston A, Gilbert HJ, Willats WGT, Knox JP (2010) Restricted access of proteins to mannan polysaccharides in intact plant cell walls. Plant J 64(2):191–203

McCartney L, Marcus SE, Knox JP (2005) Monoclonal antibodies to plant cell wall xylans and arabinoxylans. J Histochem Cytochem 53(4):543–546

Meikle PJ, Hoogenraad NJ, Bonig I, Clarke AE, Stone BA (1994) A (1-3,1-4)-β-glucan specific monoclonal antibody and its use in the quantitation and immunocytochemical location of (1-3,1-4)-β-glucans. Plant J 5(1):1–9

Melton LD, Smith BG (2001) Isolation of plant cell walls and fractionation of cell wall polysaccharides. In: Wrolstad RE (ed) Current protocols in food analytical chemistry, 1st edn. Wiley, New York, pp E3.1.1–E3.1.23

Mohnen D (2008) Pectin structure and biosynthesis. Curr Opin Plant Biol 11:266–277

Moore KJ, Moser LE, Vogel KP, Waller SS, Johnson BE, Pedersen JF (1991) Describing and quantifying growth stages of perennial forage grasses. Agron J 83:1073–1077

Pattathil S, Avci U, Baldwin D, Swennes AG, McGill JA, Popper Z, Bootten T, Albert A, Davis RH, Chennareddy C, Dong R, O'Shea B, Rossi R, Leoff C, Freshour G, Narra R, O'Neil M, York WS, Hahn MG (2010) A comprehensive toolkit of plant cell wall glycan-directed monoclonal antibodies. Plant Physiol 153:514–525

Pauly M, Keegstra K (2010) Plant cell wall polymers as precursors for biofuels. Curr Opin Plant Biol 13:304–311

Qin JP, Yang Y, Jiang JX, Yi ZL, Xiao L, Ai X, Chen ZY (2012) Comparison of lignocellulose composition in four major species of *Miscanthus*. Afr J Biotechnol 11:12529–12537

Sang T, Zhu WX (2011) China's bioenergy potential. GCB Bioenergy 3:79–90

Sarath G, Baird LM, Vogel KP, Mitchell RB (2007) Internode structure and cell wall composition in maturing tillers of switchgrass (*Panicum virgatum.* L). Bioresour Technol 98:2985–2992

Scheller HV, Ulvskov P (2010) Hemicelluloses. Annu Rev Plant Biol 61:263–289

Somerville C (2006) Cellulose synthesis in higher plants. Annu Rev Cell Dev Biol 22:53–78

Sticklen MB (2008) Plant genetic engineering for biofuel production: towards affordable cellulosic ethanol. Nat Rev Genet 9:433–443

Sun Q, Greve LC, Labavitch JM (2011) Polysaccharide compositions of intervessel pit membranes contribute to Pierce's disease resistance of grapevines. Plant Physiol 155:1976–1987

Suzuki M, Kato A, Nagata N, Komeda Y (2002) A xylanase, AtXyn1, is predominantly expressed in vascular bundles, and four putative xylanase genes were identified in the *Arabidopsis thaliana* genome. Plant Cell Physiol 43:759–767

Trethewey JAK, Campbell LM, Harris PJ (2005) (1,3),(1,4)-β-D-Glucans in the cell walls of the Poales (sensu lato): an immunogold labeling study using a monoclonal antibody. Am J Bot 92:1660–1674

Vega-Sánchez ME, Verhertbruggen Y, Christensen U, Chen X, Sharma V, Varanasi P, Jobling SA, Talbot M, White RG, Joo M, Singh S, Auer M, Scheller HV, Ronald PC (2012) Loss of cellulose synthase-like F6 function affects mixed-linkage glucan deposition, cell wall mechanical properties, and defense responses in vegetative tissues of rice. Plant Physiol 159:56–69

Verhertbruggen Y, Marcus SE, Haeger A, Ordaz-Ortiz JJ, Knox JP (2009) An extended set of monoclonal antibodies to pectic homogalacturonan. Carbohydr Res 344:1858–1862

Willats WGT, Orfila C, Limberg G, Buchholt HC, van Alebeek G-JWM, Voragen AGJ, Marcus SE, Christensen TMIE, Mikkelsen JD, Murray BS, Knox JP (2001) Modulation of the degree and pattern of methyl-esterification of pectic homogalacturonan in plant cell walls. Implications for pectin methyl esterase action, matrix properties, and cell adhesion. J Biol Chem 276: 19404–19413

Willats WGT, McCartney L, Steele-King CG, Marcus SE, Mort A, Huisman M, van Alebeek GJ, Schols HA, Voragen AGJ, Le Goff A (2004) A xylogalacturonan epitope is specifically associated with plant cell detachment. Planta 218:673–681

York WS, Darvill AG, Albersheim P (1984) Inhibition of 2,4-dichlorophenoxyacetic acid-stimulated elongation of pea stem segments by a xyloglucan oligosaccharide. Plant Physiol 75:295–297

Young RE, McFarlane HE, Hahn MG, Western TL, Haughn GW, Samuels AL (2008) Analysis of the Golgi apparatus in arabidopsis seed coat cells during polarized secretion of pectin-rich mucilage. Plant cell 20:1623–1638

Yu L, Zhou Y, Knox JP (2011) Ginseng root water-extracted pectic polysaccharides originate from secretory cavities. Planta 234:487–499